The present section highlights the literature work with focus on various process parameter that effects the grindability with special attention to surface integrity. The important process parameter that characterize the grinding operation were reviewed critically and are grinding forces, specific grinding energy, force ratio, temperature and surface roughness. Thermal induced grinding damage such as phase transformation, residual stress which effects the surface integrity of the ground surface were also reviewed in detail. Finally, the attention were shifted to literature that highlights the advancement in the field of magnetic Barkhausen noise to characterize the surface integrity of ground surface.

2.1 Grinding forces:

Grinding force is regarded as one of the most important parameters as it helps in deciding the efficiency of the grinding process. The force generated during grinding has direct influence on heat generation, tool life and on quality of machined surface. Generally, the normal grinding force is responsible for surface deformation which in turns decides the surface roughness of the ground surface whereas the generated tangential grinding force has direct influence on power consumption and also helps in monitoring the service life of the tool (Eiji, 1982). The influence of normal grinding force is very less as compared to tangential grinding force on service life of the tool. Apart from process parameter (work velocity, downfeed, wheel velocity) utilised during grinding, the magnitude of grinding force also influenced by workpiece material, grinding wheel specification (geometrical and compositional). Previous studies shows that forces generated during grinding contribute significantly to the finished product. These forces affect the surface finish, part dimension of the ground product and can also leads to higher cycle times of grinding operation (Brach *et al*., 1988).

Marshall and Shaw (1952) were one among the first who studied the grinding process in detail with special attention on grinding forces and specific energy. They depicted that increase in downfeed results into increase in tangential as well as the normal grinding force. But this rate of increase slows down after a certain value of downfeed (> 25 µm). Increase in downfeed increases the effective number of grits in contact along with the increase in maximum undeformed chip thickness (h_{max}) thereby leading to rise in grinding forces (Shenshen *et al*., 2014; Vashista *et al*., 2012). Li *et al*. (2006) shows the dependence of grinding force on maximum undeformed chip thickness (h_{max}) and observed a continuous increase in grinding force with increase in h_{max}. In a similar study performed by Kang and Huang (2017), increase in tangential grinding force were found to be larger as compared to that of normal grinding force with increasing downfeed.

Huang (2003) and Jackson *et al*. (2001) analyses the dependence of grinding forces on wheel speed. According to them, the increase in wheel speed and decrease in either downfeed or work velocity reduces the maximum undeformed chip thickness and hence reduces the grinding forces. Similarly, Huang *et al.* (2015) also noticed that with increase in wheel speed there is reduction in tangential as well as in normal grinding force and is due to heat generated in the shear zone is sufficient to plasticize the material and thereby reduces the material strength. Also there is reduction in maximum undeformed chip thickness with increase in wheel speed which also result in decreased grinding forces. However, Balan *et al.* (2016) suggested the different reason for

reduction in grinding forces with the increase in wheel speed. They reported that increase in wheel velocity leads to shift in grinding mode from ploughing to steady state and is responsible for reduction in grinding force. In contrary to the above, Ichida *et al.* (2006) observed that increase in wheel velocity during high speed cBN grinding increases the normal grinding force but it decreases the tangential grinding force.
Matsuo and Ohbuchi (1988) shows that selection of softer wheel leads to rise in normal force whereas the similar wheel with increased concentration result into smaller normal force.

Tönshoff *et al.* (1992) highlighted the effect of grit size of grinding wheel on grinding forces. They depicted that finer grit size of grinding wheel enhanced the grinding forces as it increases the effective number of grits in contact with the workpiece.

Buttery and Hameed (1977) observed that increase in work velocity and downfeed during grinding results into higher grinding forces. The increase in work velocity favours the growth of undeformed chip thickness and leads to increased grinding forces. They further observed that rise in grinding force due to increase in work velocity is gradual whereas rise in grinding force due to downfeed is severe. Similarly, Kang and Huang (2017) shows that increase in work velocity increases the normal as well as the tangential grinding force. But the increase in normal grinding force is relatively higher than the tangential grinding force. However, Marshall and Shaw (1952) proposed that increase in work velocity increases the grinding force but is found to saturate at higher work velocity.

Kopac and Kranjnik (2006) and Yao *et al.* (2014) observed that cutting speed has pronounced effect on grinding forces. They shows that increase in cutting speed reduces the contact length between individual abrasive grit and work material thereby reduces the friction, the plastic deformation and the thickness of chip removed by individual grit and hence leads to reduction in cutting forces.

In addition to the above, grinding condition (dry or flood) also influence the grinding forces (Paul and Chattopadhyay, 1995). In dry grinding, the higher grinding zone temperature generates dulling accompanied with breakage of grits and thereby enhanced the grinding force.

Komanduri (1971) shows that randomly oriented cutting grits with highly negative rake angle also increases the grinding forces. The presence of wear flats on these randomly oriented cutting grits leads to higher rubbing and ploughing and thereby increases the overall grinding forces (Malkin and Kovach, 1989).

Garrison and Garriga (1983) reported the effect of hardness of the workpiece material on the grinding force. Their study shows that as the hardness of the workpiece material to be ground increases, the material removal by ploughing decreases and hence the grinding force decreases. Huang *et al*. (2013) performed grinding of hardened steel and observed that grinding force increases with increase in carbon content of the work material. They further calculated the grinding force ratio (F_N/F_T) and noticed the larger grinding force ratio in hardened steel as compared to annealed steel.

2.2 Specific grinding energy:

Specific energy in grinding represents the energy consumed in removing unit volume of material from the work material (Shaw, 1996). Ghosh *et al*. (2008), reported that specific energy during grinding is the sum of energy involved in sliding, ploughing, chip formation and friction between trapped chip and workpiece. The percentage contribution of sliding and ploughing decreases with the increase in downfeed and thereby most of the energy is utilised in chip removal process which in turn reduces the specific energy (Malkin and Anderson, 1974). Ding *et al*. (2017) and Huang (2003) demonstrated the effect of (h_{max}) on specific energy requirement. The decrease in (h_{max}) resulted in increase of specific grinding energy. He further claims that when the value of (h_{max}) was above a critical value, the rise in specific energy was gradual whereas below the critical value the increase in specific energy was rapid. Dai *et al*. (2018) also observed an inverse relationship between (h_{max}) and specific grinding energy and is attributed to strain and strain rate hardening in grinding commonly known as 'size effect' (Heinzel and Bleil, 2007).

Blaedel *et al*. (1999) and Marinescu *et al*. (2000) depicts that specific energy requirement in case of grinding ductile material is higher than those of brittle material. This is because of fracture surface energy involved during brittle mode of material removal is smaller in comparison to energy required for plastic deformation via shearing and yielding.

Dongkun *et al*. (2015) reveals that magnitude of specific grinding energy indicates the lubricating capability of grinding fluid. Dry grinding in the absence of sufficient lubrication causes high friction between abrasive and workpiece leading to higher specific energy.

Rowe *et al*. (2003) examines the effect of grit sharpness on specific energy, in the absence of proper dressing, wheel becomes blunt and the specific energy were found to increase from 150 J/mm^3 to 400 J/mm^3.

Ramesh *et al*. (2001) reported that the increase in specific material removal rate corresponds to larger undeformed chip thickness which thereby decreases the specific energy consumed during the grinding. In case of larger chip thickness, the portion of or percentage of friction and deformation energies decreases and hence chip formation become easier (Malkin and Guo, 2008).

Rowe (2009) and Tönshoff *et al*. (1992) observed that in ductile material, removal of material mainly occurs due to elastic and plastic deformation, friction and shearing whereas in brittle material it mainly happens on account of crack formation and its propagation.

Masoumi *et al*. (2014) shows that as the downfeed increases the initial ductile mode of material removal is shifted to brittle mode and thus reduces the specific energy. They further shows that increasing downfeed increases the maximum undeformed chip thickness which again leads to reduction in specific energy.

Feng *et al*. (2009) demonstrated that decrease in work velocity and grinding depth reduces the undeformed chip thickness and hence increases the specific grinding energy. In a similar study Backer *et al.* (1952) depicts that with increase in downfeed there is gradual decrease in specific energy and is due to 'size effect'. At smaller downfeed there is reduction in chip thickness which in turns leads to high dynamic shear strength and thereby increases the specific energy. The following factor is responsible for 'size effect' in grinding (Rowe and Chen, 1997).

(1) A threshold force requirement for chip formation.

(2) New surface area created with the advancement of grit into workpiece - the sliced bread analogy. Cutting a loaf into 20 slices will take approximately twice as much energy as cutting a loaf into 10 slices even though the volume of material cut off is the same in both cases.

(3) The variation in grain shaped induced by wear and dressing action.

(4) The mechanism involved: Cutting, ploughing and rubbing.

However, at higher downfeed there is reduction in rubbing and ploughing along with the reduction in friction between abrasive grit and workpiece and hence reduces the specific energy requirement (Paul *et al.*, 1993).

Singh *et al.* (2012) performed single grit cutting test and concluded that energy variation is mainly caused by variation in ploughing energy along with the rake angle of the abrasive grit tip.

Nakayama *et al.* (1977) proposed that the poor cutting ability of the abrasive grit also increases the specific energy requirement. They shows that bluntness of the abrasive grit increases the undesirable rubbing action and also at smaller downfeed due to edge radius there is effective increase in negative rake angle of the cutting point, both of the above situation leads to increase in specific grinding energy.

Linke *et al.* (2017) in his finding observed that as the downfeed is doubled, there is increase in chip length and chip thickness by 145% and 141% respectively. This increased chip length at higher cutting depth leading to 80% reduction in specific energy. Smaller chip thickness involves higher ploughing and sliding energies. Further as the chip thickness increases the proportion involvement of these ploughing and sliding energies diminishes leading to reduction in specific energy (Shenshen et al., 2014).

Barge *et al*. (2008) highlighted the effect of wheel velocity on specific energy requirement. At smaller wheel velocity range, the increase in wheel velocity decreases the specific energy. However, at higher wheel velocity range due to increased strain rate, the increase in wheel velocity leads to increase in specific energy. Scanning electron microscopy observation of grinding chips shows that increase in wheel velocity leads to decrease in chip thickness and increase in chip length which in turn reduces the specific grinding energy (Ichida *et al*., 2006).

2.3 Grinding Temperature:

The assessment of grinding temperature is essential as it has deleterious effect on the surface integrity of the produced component which in turn affects the rate of production. According to Outwater and Shaw (1952), the higher temperature in grinding is the consequence of higher specific energy involved during the grinding process. The maximum proportion of these energy is converted into heat. In conventional machining most of the heat produced is taken away by the chips (~ 80 %) whereas in grinding major portion of the heat is conducted into the workpiece (~ 70-80 %) and thereby results into high workpiece temperature (Griffiths, 2001).These high temperature leads to various forms of thermal damage on the ground product which includes grinding burn, phase transformation, tensile residual stresses, surface cracks and reduced fatigue life (Chiu and Malkin, 1993; Malkin, 1989). Furthermore, high temperature during grinding leads to thermal expansion of the workpiece and contributes to dimensional inaccuracies in the final product. Ruisseaux and Zerkle

(1970) postulates that temperature rise in the material which is not removed (machined surface) decides the quality of the ground surface whereas temperature in the vicinity of the cutting edges of the grit removes the work material as chip and hence have no significance.

It is an accepted fact that the, grinding parameter (i.e, downfeed or depth of cut, wheel peripheral speed and table feed or work velocity) have direct effect on the maximum undeformed chip thickness (commonly known as undeformed chip thickness) which in turn have significant effect on grinding temperature (Shen *et al.*, 2014; Zhang *et al.*, 2015). Furthermore, grinding wheel specification (active grain density, grain size, sharpness of the grit) and the characteristics of workpiece material also influence the grinding temperature (Yamamoto *et al.*, 1977).

Generally, increase in material removal rates which occur due to increase in undeformed chip thickness leads to higher heat generation during grinding process. As the undeformed chip thickness is over the critical value (> 0.75 μm) during grinding of Inconel 718, then in the contact zone heat flux becomes more than the critical value. Under such condition, the cutting fluid reached in the film boiling state (from liquid phase to gaseous phase) and heat conduction capability of fluid decreases to near 30 times thus favouring the sudden rise in temperature (Ding *et al.*, 2017).

Yao *et al.* (2014) during grinding of Aermet steel using cBN and alumina wheel observed that as the work velocity increases, the input power increases leading to more heat generation per unit time and thus increases the grinding temperature. Furthermore, as downfeed increases more number of abrasive grit play their role in cutting and thus increases the grinding force which significantly increases the plastic deformation and friction leading to more heat generation and thereby increase the grinding temperature (Mahamani and Jawahar, 2018). Similarly, Kitajima *et al.* (1992) observed that with increase in tangential grinding force there is continuous increase in grinding temperature.

Further, Lin *et al.* (2016), demonstrated that heat source movement in grinding increases with increasing work velocity which thereby reduces the time that the moving heat source spent with the workpiece and most of the heat generated gets transferred quickly into the atmosphere leading to reduced grinding temperature.

Rowe *et al.* (1997) predicts that characteristics of abrasive grit (sharpness, shape, grit density) and its interaction with workpiece significantly affect the heat generation, sharp grit result into lower heat generation and vice versa (Zhu *et al.*, 2013). Khan *et al.* (2018) predicted that the influence of downfeed and table feed upon temperature is not similar under all different environment. In dry grinding condition, downfeed has more significant effect on temperature as compared to table feed whereas during wet grinding the increase in temperature is rapid at higher value of table feed. However, temperature attained in dry grinding is higher as compared to wet grinding. This is due to high specific energy associated with dry grinding as it involves grain sliding and shearing with adverse abrasive grit shape and size, albeit in wet grinding, the effective cooling and lubrication of cutting fluid reduces the grinding temperature (Tawakoli *et al.*, 2009).

It is already established that, energy input during grinding is a function of process parameter, wheel condition, lubrication etc. and is thereby an uncontrolled output. As temperature generation during grinding is directly related to the energy consumption, it is also difficult to control the temperature. The utilization of thermocouple technique in estimating grinding temperature is rather difficult because of large thermal gradient in time and space nearby the ground surface (Snoeys *et al.*, 1978; Zhu *et al.*, 1995). Furthermore, temperature measurement using thermocouple technique is not so practical as it is restricted to laboratory and cannot applied to real production environment (Malkin, 2007). In process measurement of the energy input during the grinding process along with the thermal analysis provide a better approach in estimation of grinding temperature.

Various researcher performed the thermal analysis to predict the transient temperature during grinding process (Beirmann and Schneider, 1997; Guo and Malkin, 1995). Numerical modelling and its analytical verification in estimating grinding temperature in shallow and deep grinding was performed by (Anderson *et al.*, 2008). Furthermore, Shaw (1994) performed the thermal analysis to predict the grinding temperature in terms of process parameter. From the above model, he observed that increase in either of wheel velocity or downfeed led to increase in grinding temperature. Later on, Malkin and Guo (2007) confirms the applicability of the model in estimating grinding zone temperature.

2.4 Surface Integrity:

The term "surface integrity" was used in early 1960 to describe the behaviour of the machined surface which includes both surface topography and near surface damage (Field and Kahles, 1964). Surface integrity can be technologically defined as the combination of various properties (superficial and near depth) of machined surface that effect the performance of the surface during real engineering application (Davim, 2010). Surface integrity includes the measurement of surface topography (such as surface texture, surface roughness, and waviness), mechanical parameter (hardness, residual stress, fatigue strength) and metallurgical alteration (phase transformation, microstructure, grain size) (Ulutan and Ozel, 2011). Fredj and Sidhom (2006) observed that higher temperature involvement in grinding leads to various sorts of thermal damage on the ground component. Thermal damages usually occur in the form of surface burn, phase transformation, induction of tensile residual stresses, surface cracks, reduced fatigue life, thermal distortion and inaccuracies (Malkin, 1989). The forthcoming section gives the detail review of the surface integrity, measurement technique, and the factor influencing.

2.4.1 Surface Roughness:

Grinding process are usually selected for final finishing of components as it is capable to satisfy stringent requirements of surface roughness and tolerance. Higher surface roughness is associated with deeper grooves on the surface which acts as site for local accumulation and concentration of chloride ions leading to stress corrosion cracking, thereby assessment of surface roughness is important (Shoji, 2003).Various studies were performed in the past to predict the surface roughness of the ground workpiece in terms of wheel topography and the process parameter. Theoretically calculated surface roughness is of limited practical use as it is necessary to evaluate relative influence of process parameter on the roughness for which empirical relation needs to be used (Malkin and Guo, 2008).

Surface roughness is dependent on abrasive grit size, finer size abrasive grit produce lesser rough surface as compared to higher size abrasive grit. Yossifon and Rubenstien

(1982) during grinding of stainless steel using alumina wheel observed an improvement in the surface roughness with increase in wheel hardness grade. The continuous wear of the wheel alter its topography and thereby surface roughness also changes with time, and this is observed during longer grinding cycle with less frequent dressing. They observed that surface roughness of the ground stainless steel is smaller when the grinding is performed with fine dressed wheel. However, when the grinding wheel undergo coarse dressing, the complete grains gets pull out of the surface and thereby number of active grains gets reduced which hence, enhance the roughness (R_a) of the workpiece.

In addition to grinding wheel topography, workpiece characteristics along with the machining parameter also have significant influence on the surface finish (Malkin, 1989). Tso (1995) investigated the role of process parameter (wheel velocity, work velocity and downfeed) on surface finish. The result shows that with increase in work velocity and downfeed, surface finish gets deteriorated whereas increase in wheel velocity led to improvement in the surface finish. Similarly, Ichida *et al.* (2006) also concluded that surface roughness decreases with increase in wheel velocity and is due to reduction in side swelling of groove formed with increase in wheel velocity. Alternatively, Chakrabarti and Paul (2008) carried out the simulation of the surface topography to investigate the effect of machining parameter on surface roughness. They simulation predict a significant improvement in the surface finish with increase in wheel velocity, diameter of the wheel and abrasive grit density. Also, they observed that increase in work velocity result into poor surface finish. Huang *et al.* (2015) also observed a similar variation in surface roughness with increase in wheel speed. They depicted that at higher wheel speed grinding surface scratch depth becomes smaller resulting into improved surface finish.

In the grinding process, during interaction of abrasive grit with the workpiece, the grit initially slides without performing any cutting of the workpiece due to elastic deformation of the system which is recognized as rubbing phase. Further, as the stress between grit and workpiece is increased beyond the elastic limit, plastic deformation occur and is known as ploughing phase where work material piles up to the front and sides of the grit to form a groove which in turn have significant effect on the surface finish. Tawakoli *et al.* (2009) performed grinding operation on 100Cr hardened steel and noticed that surface finish in wet grinding is finer as compared to dry grinding. Dongkun *et al.* (2015) observed an 11% reduction in R_a value during wet grinding as compared to dry grinding. The effective lubrication in wet grinding, force the chips generated to slide easily over the tool surface and hence leads to finer surface finish. Zhou *et al.* (2016) observed that the presence of lubricating medium decreases the magnitude of friction between abrasive grit and workpiece surface leading to improved surface finish with no surface defect. However, reuse of the grinding lubricant containing small particles of grinding chips and abrasive may produce surface indentation.

Kitajima *et al.* (1992) studied the effect of material hardness on surface roughness, they noticed that increasing material hardness restrict the formation of bulge on the side edges and hence produce better surface finish. Zhang *et al.* (1995) during grinding of silicon carbide and silicon nitride found that increase in surface roughness before grinding decreases the specific energy requirement because brittle mode of fracture needs less energy so that a larger surface roughness corresponds to smaller specific energy.

Furthermore, surface roughness increases when the fracture mechanism dominates in the material removal process.

2.4.2 Microstructure and microhardness:

High heat generation in grinding owing to high specific energy involvement results into higher grinding temperature. The intensity of heat generation in grinding is not only dependent on interaction forces rather it is also significantly influenced by plastic deformation mechanism associated with material removal process, work velocity, and wheel speed. The high temperature of the workpiece when followed by rapid cooling causes phase transformation and generally termed as metallurgical damage. Theses damages are often characterized as tempering of hard martensitic phase, formation of hard and brittle martensitic phase (termed as white layer) along with the change in surface hardness. Mao *et al.* (2011) discussed the formation mechanism of white layer and concluded that the three key mechanism are responsible for the white layer formation (1) rapid heating and quenching (2) severe plastic deformation resulting into homogeneous structure with very fine grain size (3) surface reaction with environment. Akcan *et al.* (2002) believed that the rapid heating and subsequent quenching have predominant effect on the white layer formation. Huang *et al.* (2015) noticed the formation of white layer at different wheel speed during high speed grinding. They discussed that in high speed grinding the formation of white layer is mainly due to rapid heating and quenching of the workpiece and not because of cold plastic deformation as magnitude of plastic deformation in high speed grinding is very small as compared to low speed grinding as grinding force reduces with the increase in wheel speed.

During grinding of AISI 52100 hardened steel, the white layer appears in a direction perpendicular to the grinding direction. The white layer is composed of α-phase (requenched martensite), α-phase (tempered martensite), fine recrystallized γ_R phase (retained austenite) along with secondary phases of Fe_3C, Fe_3O_4 and FeO whereas dark layer which occur just beneath the white layer is composed of α- phase, precipitated Fe_3C phase and sorbate structure (Eda *et al.*, 1981). Higher hardness of white layer is attributed to formation of untempered martensite (Guo and Sahni, 2004). Gupta *et al.* (1997) shows that workpiece at higher temperature when undergoes sudden quenching forms hard and brittle martensite whereas tempering burn causes the softening of the surface due to the formation of tempered martensite.

Madopothula *et al.* (2017) observed the formation of white layer of thickness 56µm during grinding of AISI 52100 steel using sol-gel alumina wheel. But, no white layer is observed when grinding is performed with fused alumina grinding wheel. The formation of white layer is dedicated to high toughness of sol-gel alumina wheel which led to generation of wear flats with increasing grinding passes and thereby shift the dominant grinding mechanism from shearing to ploughing and sliding hence increases the grinding temperature. Sosa *et al.* (2007) while performing grinding of thin wall ductile iron plates observed no phase transformation in the ground specimen as the temperature generated is not sufficient to cause phase transformation. Similarly, Silva *et al.* (2007) also observed no alteration in the subsurface of the ground sample under different grinding condition and is due to magnitude of heat generated and plastic deformation is not sufficient to cause alteration in the subsurface microstructure.

Liu *et al.* (2015) found that, at constant downfeed and feed rate, number of grinding passes also have significant effect on the thickness and mechanical properties of the hardened layer. Shi *et al.* (2006) performed modelling of white layer and observed that lubrication medium and mode, abrasive type, downfeed and cutting speed all contribute significantly in the formation of white layer.

Tomlinson *et al.* (1991) studied the effect of machining parameter on white layer formation during grinding of EN 24 steel and concluded that increase in downfeed and decrease in wheel velocity or work velocity generates thicker white layer. However, Huang *et al.* (2015) observed an increase in the thickness of white layer with increase in wheel velocity during grinding of AISI 52100 hardened steel. Increase in downfeed induces more heat flux in the workpiece surface during grinding giving rise to more thick white layer (Zarudi and Zhang, 2002). However, increase in work velocity produce shallower heat penetration due to reduction in heating time which thereby reduces the depth of thermally affected layer (Malkin and Guo, 2007). Huang *et al.* (2013) observed similar variation in the thickness of white layer with downfeed, wheel speed and work velocity. The thickness of white layer increases with the increase in wheel speed and downfeed whereas with increases in work velocity the thickness of white layer first increases and then starts to decrease at higher work velocity.

Yang *et al.* (1996) studied the wear resistance of the white layer formed during machining. They shows that presence of white layer decreases the wear resistance of the material. The large deformation transition between the white layer and matrix led to the formation of microcracks. These cracks may get propagated along the interface between the unaffected matrix and the white layer and causing delamination of the white layer. Mao *et al.* (2011) characterize the hardness of the white layer formed during grinding of hardened steel and annealed steel. They noticed that the hardness of the white layer formed on hardened steel is greater than those of white layer formed on annealed steel. The hardened steel prior to machining contains some amount of retained austenite whereas no austenite is present in annealed steel. This retained austenite led to more martensite formation upon heating and quenching of the workpiece and hence causes more hardness (Krauss, 1990). In a similar study, Huang *et al.* (2013) noticed that the thickness of white layer increase with increase in carbon content of the workpiece material. The intermediate phase between Fe and Fe_3C which enhances the formation of austenite, increases with the increase in carbon content of the workpiece. During the same time, more carbon gets diffuse into the austenite and enhanced the formation of martensitic phase.

Brockhoff (1999) investigated the effect of feed speed on grind hardening of SAE 4140 steel using alumina wheel. The increase in feed speed gives rise to larger grinding forces which in turn increases the power consumption. Higher grinding power generate higher temperature thereby increases the thickness of hardened layer. In contrary, the increase in table feed reduces the thickness of the hardened layer and is due to reduction in contact time between abrasive grit and workpiece and hence less time is available for heat to get conducted into the workpiece. He further noticed that depth of hardened layer is maximum at medium feed speed (0.01m/min < feed speed< 5m/min) as at very low feed speed (feed speed = 0.01m/min) the specific energy is high but power consumption is low hence reduces the heat generation and at very high feed speed (feed speed = 5m/min) power consumption increases but contact time decreases hence very low heat can get conducted into the workpiece reducing the depth of hardened layer.

Sullivan *et al.* (2004) and Thompsan and Tanner (1994) noticed that hardness of the ground surface increases with the increase in plastic deformation. At lower downfeed, the changes in the microhardness in not significant but at higher downfeed noticeable increase in hardness is observed and is due to grain refinement, phase transformation and plastic deformation (Eda *et al.*, 1993; Sosa *et al.*, 2007). However, all three mechanism may not observed in grinding simultaneously. Eda *et al.* (1993) observed the presence of grain refinement and phase transformation during grinding of medium carbon steel, whereas Sosa *et al.* (2007) noticed the existence of plastic deformation and did not observed any phase transformation.

2.4.3 Residual stress:

Residual stress is defined as the stresses that left inside a material after material processing and manufacturing when all external force or thermal gradient is removed. The grinding process invariably led to the formation of residual stress in the vicinity of the ground surface which can significantly affect the performance of the product under real service condition. The properties which are greatly influenced by the residual stress are fatigue life, fracture strength, distortion, dimensional stability, corrosion resistance etc. (Totten *et al.*, 2002).

Marshall and Shaw, 1952 shows that residual stress in the ground material is due to temperature gradient and is tensile in nature. According to Colwell *et al.* (1955) the thermomechanical condition during the grinding process is responsible for generation of tensile residual stress. Snoeys *et al.* (1978) reported that the plastic yielding of the surface layer of the workpiece is responsible for tensile residual stress. In reverse, Helieby and Rowe (1982) noticed that the phase transformation is the primary factor responsible for the tensile residual stress.

In grinding process, the generation of residual stress is attributed to the combined effect of mechanical deformation, thermal gradient and the phase transformation of material (Zhang *et al.*, 1992). Mechanical interaction between abrasive grit and the work material lead to the generation of residual compressive stress owing to localized plastic flow (Mahdi and Zhang, 1996). Higher grinding temperature results into thermal stress and often leads to generation of tensile residual stress. During grinding, the heated material in the grinding zone close to the surface expand whereas the cooler subsurface material restrict this expansion, this tendency give rise to generation of compressive residual stress near the surface. Further, if the generated compressive stress is large enough, it causes plastic flow of the material under compression and during cooling deformed material wants to be shorter than the subsurface material and hence causes tensile stress to develop near the surface (Mahdi and Zhang, 1997). Moreover, if the ground material experiences a critical temperature followed by immediate cooling then phase transformation takes place, which also lead to the formation of additional tensile residual stress. When phase transformation involves formation of martensite then compressive residual stress will be generated as specific volume of martensite is higher than that of ferrite. Nguyen *et al.* (2007) also observed that martensitic transformation favours the generation of compressive residual stress as body centred tetragonal (BCT) lattice of martensite occupies larger space than the body centred cubic lattice of ferrite. Moreover, they further predict that precipitation of interstitial carbide Fe_2C and $Fe_{2.4}C$ reduces the volume of body centred martensite lattice and hence led to the generation of tensile residual stress. However, if sufficient amount of austenite is retained in the workpiece then it leads to the generation of the tensile residual stress as specific volume of austenite is lower than that of ferrite (Zhang and Mahdi, 1995).

Tempering burn or Overtempering during the grinding process takes place below the austenizing temperature and is associated with the transformation of body centred tetragonal into body centred cubic ferrite and is therefore induces tensile residual stress in the ground surface (Balart *et al.*, 2004).

Brinksmeier (2003) studied the effect of process parameter which have significant influence on the residual stress state of the ground surface. He found that increase in downfeed increases the material removal rate along with the grinding power causing more thermal loading and hence compressive residual stress state of the ground surface gets shifted to tensile residual stress. He further noticed that grinding with cBN wheel induces compressive residual stress at the surface because of good thermal conductivity and effective chip formation capability of the wheel (Zhejun *et al.*, 1989). Further, the magnitude of this compressive stress with cBN wheel increases with increase in surface hardness of the workpiece (Abrao and Aspinwall, 1996). However, increasing grain size of the abrasive grit is beneficial as it shifts the tensile residual stress to compressive stress. In his another study Brinksmeier *et al.* (1982) observed that fine dressing although gives rise to higher surface finish as compared to coarse dressing but it results in higher thermal load and hence produce higher tensile stress on the workpiece surface.

Tarasov *et al.* (1989) during grinding of hardened steel discussed that the generation of surface residual stress is mainly influenced by wheel condition, downfeed and lubricating medium. The utilization of oil as a lubricating medium is more effective in reducing coefficient of friction between abrasive and workpiece as compared to water based coolant, thereby using oil as a lubrication medium generates lower tensile residual stress (Neailey, 1989). Paul and Chattopadhyay (1995) studied the effect of downfeed on surface residual stress and observed that increase in downfeed enhances the surface tensile residual stress owing to increase in temperature. Similarly, Fredj *et al.* (2006) during conventional grinding of AISI 304 steel noticed that the increase in downfeed or work velocity give rise to more and more accumulation of surface tensile residual stress. Tonshoff *et al.* (1992) acknowledged that the information regarding residual stress helps in predicting hardness change and phase transformation occurred during the grinding process. Brinksmeier and Tonshoff (1985) studied the influence of grit size on residual stress while performing grinding experiment with cBN wheel. Their study claims that large grit size leads to increase in grinding forces as the more number of larger grits get flattened during dressing hence heat generated owing to friction increases and thus leads to the formation of undesirable residual stress. Apart from above, material hardness also have profound effect on surface residual stress, material with higher hardness generates more compressive residual stress on the surface of the ground surface during grinding with cBN wheel (Herzog *et al.*, 1988).

Recently, Zhou *et al.* (2016) noticed that grinding using 60# grit size produce higher residual stress with higher penetration depth as compared to 180# grit size. Naskar *et al.* (2018) studied the effect of lubrication mode during grinding of Inconel 718 with cBN wheel and observed that higher heat transfer coefficient under flood cooling further reduces the intensity of tensile residual stress. Azarhoushang *et al.* (2017) found that extent of thermal damages of the workpiece can be reduced by using structured wheel during dry grinding. They further shows that radial infeed (workpiece oversize) have large influence on the temperature generated during dry grinding. Increase in radial infeed increases the grinding contact length which in turn causes more heat generation and hence favours the generation of undesirable tensile residual stress. Aurich and Kirsch (2013) performed the grinding using slotted grinding wheel and concluded that such wheel enhances the cooling efficiency as compared to other utilized wheel and thereby reduces the occurrence of thermal based tensile residual stress.

2.4.3.1 X-ray diffraction method for assessment of residual stress:

Assessment of residual stress using X-ray diffraction involves the measurement of angles at which maximum diffracted intensity happens when a crystalline material is subjected to X-rays. These angles were utilised to predict the interplanar spacing of the diffraction plane with the help of Bragg's equation. In the presence of residual stress the interplanar spacing will be different than those of unstressed state and the difference is proportional to the magnitude of residual stress present in the sample. As per Gazzara (1983) residual stress can be either of tensile or of compressive nature. He utilized the concept of peak shift to determine the state of residual stress state that exist within the sample. Under the presence of compressive residual stress, the initial position of the atoms (without stress, i), get reduced from d_i to a smaller separation d_f (final stress state, f). Now as per Bragg's law this correspond to an increase in θ (the angle at which diffraction takes place). Similarly, in the presence of tensile residual stress, the initial position of the atoms (without stress, i), get increased from d_i to a larger separation d_f (final stress state, f), which further leads to decrease in θ as per Bragg's law (refer Fig.3.6). From the above study, it can be seen that the stress state of a sample can simply be known by studying the nature of peak shift, a rightward shift of the peak position shows the presence of compressive residual stress whereas leftward peak shift denotes the presence of tensile residual stress. More and more peak shift as compared to unstressed state shows more and more accumulation of residual stress. However, it is difficult to tell the actual magnitude of the residual stress present within the sample, for which the $\sin^2\Psi$ technique is used. In this technique a graph is plotted between 2θ and $\sin^2\Psi$, which is then fitted with a straight line, the slope of which gives the magnitude of the residual stress. The mathematical relation for $\sin^2\Psi$ technique is given below.

$$\sigma = \frac{E}{(1+ \nu)\, Sin^2\Psi} \, \frac{cot\theta}{2} \{\Delta 2\theta\} \tag{2.1}$$

Where, σ = magnitude of stress to be determined

E = Young's modulus of crystallographic plane

ν = Poisson's ratio of the material under examination

θ = peak position

$\Delta 2\theta$ = change in peak position

Ψ = is the angle between the surface normal and the bisector of source and diffracted X-ray beam

2.4.3.2 Need of fast assessment of residual stress.

The common problem that is associated with the X-ray diffraction measurement technique is to determine precise location of diffraction peak which requires accurate sample alignment and precise method to locate the diffraction peak. Another limitation is linked with the size of the sample and its geometry as with irregular geometry it is difficult to get clear diffraction data. The method is equally applicable to isotropic and anisotropic material but it is necessary to have homogeneous strain distribution. The oscillatory behaviour of the sample shows the occurrence of inhomogeneous strain distribution, which if analysed in a similar fashion as the case under homogeneous strain distribution will cause a significant error in the final result. The assessment of stress using XRD technique is further gets complicated due to scattering, broadening and varying background levels of X-ray (Tonshoff and Brinksmeier, 1980).

Further, higher initial cost along with the long analysis time restrict its application in real time testing. Assessment of subsurface residual stress distribution is again time consuming as it requires subsequent electro-polishing and then again clamping. Conventional/Regular testing methods which includes metallographic inspection, scanning electron microscopy, X-ray diffraction and microhardness measurement were frequently used to assess the surface integrity of the ground surface. However, conventional methods being laboratory based cannot be used for real time testing (Brinksmeier *et al.*, 1984; Inasaki *et al.*, 1993). Also, determination of depth profile using residual stress require electrolyte polishing to remove layer and may cause changes in the stress profile (Balart *et al.*, 2004).

Hence, despite of above well-established method grinding industry still looks for fast, reliable and economic technique to detect the grinding damage at the rate of production. Brinksmeier *et al.* (1984) shows that surface integrity including (microstructure, microhardness, and residual stress) can be assessed using magnetic technique. The basis of measurement lies in the fact that magnetic parameter are very sensitive towards changes in the above surface integrity. Further, the measurement using magnetic technique is cost effective, fast, environmental friendly and can be automated for online monitoring (Inasaki *et al.*, 1993). Similarly, Gupta *et al.* (1997) utilised magnetic technique (Barkhausen noise technique) to detect the grinding damage. They shows that characterization of alteration in microstructure using conventional etching method is quite time consuming. In comparison, Barkhausen noise technique is a fast, reliable and non-destructive in nature. In line with above, Lindgren and Lepisto (2002) also advocated the use of Barkhausen Noise technique in the assessment of residual stress. They predicted that use of hole drilling and XRD technique in the measurement of residual stress involves higher capital, higher measurement time and also it is not suitable for large components. Contrary to that, Barkhausen Noise technique is fast, reliable, cost effective, environmental friendly and easy to be automation technique.

2.4.3.3 Magnetic Barkhausen Noise technique:

Barkhausen noise also known as Magnetic Barkhausen Noise is discovered in 1919 by German physicists Prof. Heneinrich Barkhasuen. The generation of noise was first experienced by hearing the sound generated in headphones which is linked to a pick up coil which are wrapped around a ferromagnetic material, as the material gets gradually magnetized (Barkhausen, 1919). However, Tiitto (1970) was the first to draw the attention of the method in industrial application (Tiitto, 1977). A clear understanding of the magnetization process of the ferromagnetic specimen were possible with the effort of French scientist Pierre Weiss who in 1907 observed that in order to minimize magnetostatic energy ferromagnetic material divide itself into magnetic domain. Felix Bloch showed that each magnetic domain is separated from its neighbours by finite frontier called as domain walls or bloch walls. Generally, two types of domain wall exists i:e 180^{o} domain wall and 90^{o} domain wall depending upon the crystallographic arrangement of the ferromagnetic material. However, it is 180^{o} domain wall which are responsible for the generation of Barkhausen noise as its mobility is higher as compared to 90^{o} domain wall. Domain wall which are antiparallel to each other are termed as 180^{o} domain wall while those which are perpendicular to each other are termed as 90^{o} domain wall (Chikazumi, 1964). The two types of domain wall are depicted in Fig.2.1. Cullity (1972) shows that in the absence of external magnetic field the direction of these magnetic domains are random resulting in zero net magnetization as shown in Fig.2.2 (a). However, under externally applied magnetic field domains with the direction close to the applied magnetic field increases their size at the cost of less favourable domain which leads to increase in magnetization of the specimen Fig.2.2 (b).

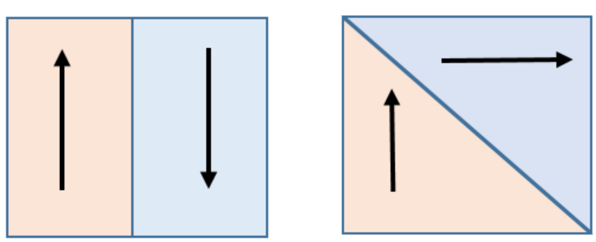

(a) (b)

Fig.2.1 Arrangement of magnetic domain in (a) 180^{o} Domain Wall (b) 90^{o} Domain Wall

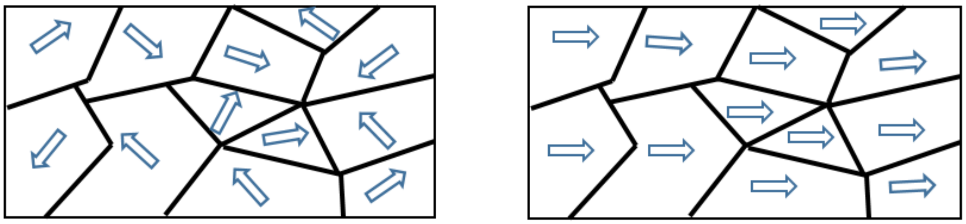

(a) (b)

Fig.2.2 (a) Domain in the absence of magnetic field (b) Arrangement of domain after magnetization

Once the applied magnetic field is increased enough there exists only one domain inside the ferromagnetic sample in a direction parallel to the applied field which corresponds to saturation magnetization (B_s), beyond which any further increase in magnetic field will result in little or no magnetization (Durin and Zapperi, 2006; Jiles, 1991).

However, decrease in magnetic field strength after the saturation magnetization result into decrease in magnetization of the sample, but the path of this decreasing magnetization is different from those of increased magnetization and the difference in the path is what is known as magnetic hysteresis. As the value of applied field strength is reduced to zero, there is still some sorts of magnetization left in the sample and this left out magnetization is known as remanence (B_R). The further increase in applied field strength in the opposite direction leads to further decrease in magnetization of the material, and the value of applied field strength at which magnetization of the ferromagnetic sample reduced to zero is termed as coercivity (H_C). Now if the applied field strength is further increased, the magnetization of the sample again gets saturated but in the opposite direction. The decrease in applied external field, then reversing it and again increasing it result into the formation of hysteresis loop as shown in Fig.2.3 (Anderson *et al.*, 1990).

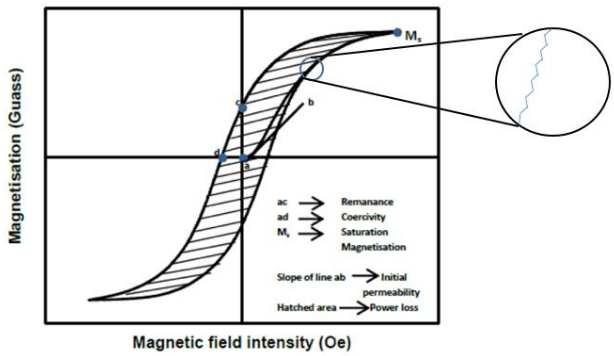

Fig.2.3 A typical hysteresis loop formation (Srivastava *et al.* 2017)

Although, the applied magnetic field varies smoothly and the resulting hysteresis loop observed to be smooth, but this is not true as domain wall motions are jerky and discontinuous in nature and the same can be seen from Fig.2.3. This happens due to presence of pinning sites within the material. The pinning sites restrict the motion of domain wall and the extent of which is depend upon the strength of the pinning sites. Further, when the applied external field is strong enough to overcome the barrier imposed by pinning sites, they abruptly and irreversibly break away from the pinning sites. These process thereby causes sudden changes in the magnetization of the material and leads to the noise like signal termed as Barkhausen noise (Jiles, 2000). Generally, there are three different mechanism involves in generation of Barkhausen noise (Jiles, 1988). These are

(i) Irreversible discontinuous domain wall bowing

(ii) Irreversible discontinuous domain wall translation

(iii) Irreversible discontinuous domain wall rotation

When the magnitude of applied magnetic field is small, domain wall bowing is a reversible process in which the domain wall gets stretched like an elastic membrane.

However, the process becomes irreversible as the domain wall gets sufficiently deformed and the expansion continues without further increase in applied magnetic field strength causing sudden changes in magnetization and thereby generate Barkhausen noise. Irreversible domain wall translation contribution is largest in the generation of Barkhausen noise. This happens when domain wall breaks away from the pinning sites under high applied magnetic field leading to sudden changes in the magnetization. Irreversible domain rotation occur when the magnetic moment inside the domain rotate from their initial easy axis to another crystallographic axis closest to the applied field direction. This switching of moments from one easy axis to another causes change in magnetization and result into generation of noise.

The pinning sites which hindered the motion of domain wall are the inhomogeneities which may be in the form of grain boundaries, second phase material, inclusion etc. present within the material (Cullity, 1972). Microstructural features such as impurities, crystal defects, grain boundaries, and dislocations or even applied or residual stress acts as the pinning sites and thereby, hinder the domain wall motion which ultimately effects the MBN signal (Blaow *et al.*, 2005; Gurruchaga *et al.*, 2010; Ktena *et al.*, 2014; Moorthy *et al.*, 2003). In an attempt to characterize the various properties of material, number of parameter derived from the Barkhausen noise were utilized in the literature. The frequently used parameters are events per magnetizing cycle, root mean square voltage, peak to peak voltage, MBN energy, peak position, width and height of MBN profile (Ghanei *et al.*, 2014; Mitra *et al.*, 1995).

The dependence of Barkhausen noise on above mentioned mechanical and metallurgical properties enables the wide spectrum application of the technique to the manufacturing industry which includes, automobile industry, aerospace industry and heat treating where it can be used to sort defected component, to control microstructure, to assess service life and in service damage of the component. However, Moorthy *et al.* (2005) and Wilson *et al.* (2009) highlighted the limitation of the Barkhausen noise technique in the sense that it can only be used to detect changes in the very near to the surface region of the material. The depth of penetration of the MBN signals can be thought of governed by same skin depth equation of electromagnetic field (Moorthy *et al.*, 2003). Mathematically,

$$\delta = \frac{1}{\sqrt{\pi f \sigma_m \mu_0 \mu_r}} \tag{2.2}$$

Where, f - frequency of excitation

σ_m - conductivity of the material

μ_o - permeability of vacuum

μ_r - relative permeability of material

Generally low frequency excitation (<1 Hz) is used for detection of MBN signal from deeper subsurface, in contrary high frequency excitation (>10 Hz) is used for characterizing changes in near- surface properties, by limiting the MBN signals from subsurface due to eddy current damping (Moorthy *et al.*, 2005; Moorthy, 2016). In the literature, it was observed that both type of waveform (sinusoidal and triangular) of the magnetic field is used in the Barkhausen noise technique. However, it is advantageous to use triangular waveform in comparison to sinusoidal waveform (Durin and Zapperi, 2006).

Gauthier *et al.* (1998) and Blaow *et al.* (2007) pointed out the difficulties in the assessment of residual stress using Barkhausen noise technique. According to them, apart from residual stress microstructural composition, hardness of the material and other unmeasured properties also effects the generation of Barkhausen noise signal and it is quite difficult to distinguish the effect of different material properties from the signal. Additionally, the direction of measurement also have significant effect on the signal and thereby should be taken into account during the measurement using Barkhausen noise technique. Hence, in order to evaluate residual stress effectively using this technique, the measurement device should be calibrated against the material under investigation.

Jiles (2000) reported the influence of grain size on Barkhausen noise emission. As the grain size becomes smaller, the number of magnetic domains and domain walls increases which result into higher Barkhausen jumps but of smaller amplitude. The increase in grain size shift the peak position of Barkhausen envelope to lower applied field strength (Moorthy *et al.*, 1997). Ng *et al.* (2001) studied the influence of carbon content on three parameter of Barkhausen noise namely FWHM (Full width at half maximum) of the envelope, the slope and the root mean square value. They noticed the continuous increase in all the above stated parameter with increasing carbon content. On the other hand, Pal'a and Bydzovsky (2013) examines the influence of grain size on the peak value of the Barkhausen noise envelope. They shows that peak height of the Barkhausen noise increases as the grain size increases from 28µm to 46µm.

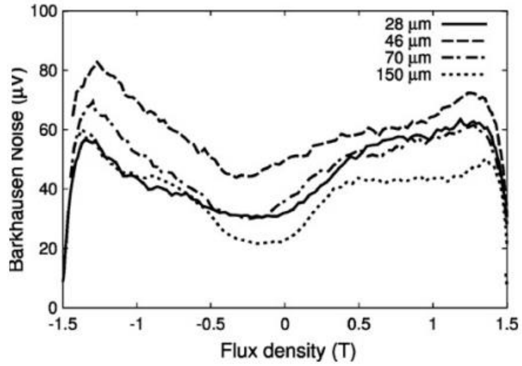

Fig.2.4 The influence of grain size on peak height of Barkhausen noise (Pal'a and Bydzovsky, 2013)

The further increase in grain size from 46µm to 150µm result into decrease in peak height as shown in Fig.2.4 and is due to decrease in number of domain and hence domains walls with increasing grain size.

Sipahi (1994) shows that increase in hardness of the material result into increase in pinning sites (dislocation density) which restrict the motion of domain wall and thereby leads to lower Barkhausen noise activity. The root mean square value of the BN signal also found to decrease with increasing hardness (Santa-aho *et al.*, 2009) whereas a linear relationship was noticed between inverse of root mean square value and hardness of the ferromagnetic sample (O' Sullivan *et al.*, 2004). The coercivity value derived from the hysteresis loop can also be used to predict hardness of the material. The increasing hardness of the material correspond to higher coercivity (Kinser *et al.*, 2005). However, Meszaros and Szabo (2005) reported that changes in peak position can precisely predict the hardness change while performing the measurement on dual phase steel. Recently, Deng *et al.* (2018) studied the effect of tempering temperature on Barkhausen noise parameter (peak value and RMS). Under no-tempering condition, the higher hardness of the material is attributed to presence of martensitic phase in the microstructure which acts as an effective pinning sites for domain wall motion and hence result into lower Barkhausen noise activity and thus reduces the peak value and RMS value. However, as the tempering temperature increases the martensite starts to decompose into bainite and other phases which being soft provide less hindrance to domain wall motion hence leading to higher peak value and RMS value of Barkhausen noise as shown in Fig.2.5.

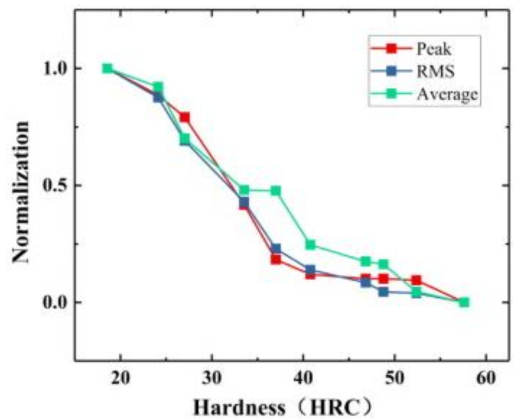

Fig.2.5 The variation in Barkhausen noise parameter with tempering induced hardness change (Deng *et al.*, 2018)

In addition, they also observed that surface roughness of the component has a major contribution in the generation of Barkhausen noise signal.

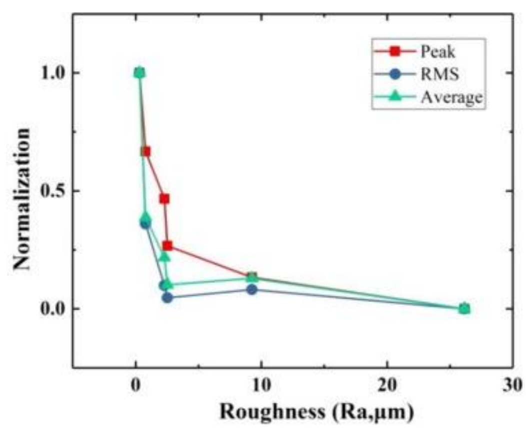

Fig.2.6 The influence of surface roughness on Barkhausen noise parameter (Deng *et al.*, 2018)

With the increase in surface roughness of the sample a reduction in the peak and RMS value of the signal is observed as shown in Fig.2.6. This is due to the fact that increasing surface roughness expands the spacing between domain wall hence its movement becomes difficult.

Tiitto (1977) observed that the amplitude of the Barkhausen noise signal is influenced by the stress and also by the applied magnetic field. He noticed that tensile stress and the applied magnetic field have similar effect on the magnetic domain, both of these factor enhance the generation of Barkhausen noise signal. In opposite to above, compressive residual stress and applied external magnetic field have conflicting effect and thereby leads to reduced level of Barkhausen noise signal.

Gauthier *et al.* (1998) studied the correlation of BN energy with residual stress measured using hole drilling technique and X-ray diffraction. They observed that BN energy increases with increase in tensile residual stress and decreases with increase in compressive residual as shown in Fig.2.7 (a). Similarly, Kleber and Vincent (2004) also noticed the similar variation in root mean square (rms) value of the Barkhausen noise signal and the residual stress. They observed that increase in tensile residual stress increases the Barkhausen noise signal whereas increase in compressive stress reduces the Barkhausen noise. The correlation between residual stress and Barkhasuen noise is shown in Fig.2.7 (b).

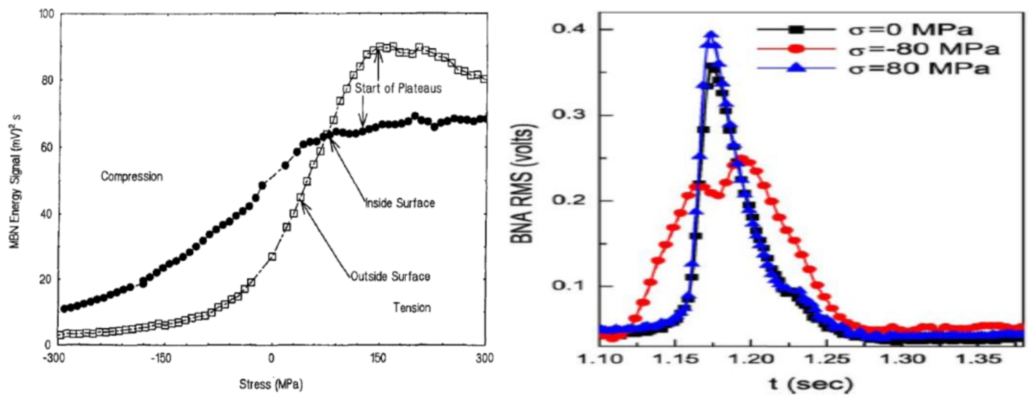

Fig.2.7 (a) Correlation between MBN energy and residual stress (Gauthier *et al.* 1998) (b) The effect of residual stress on BN (rms) value (Kleber and Vincent, 2004)

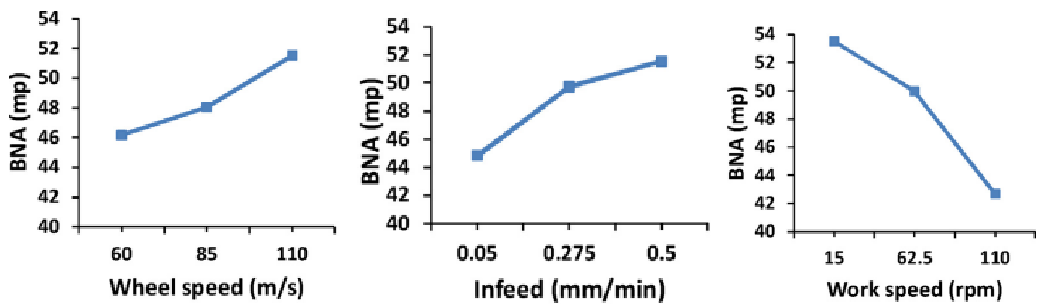

Fig.2.8 The effect of grinding process parameter on Barkhausen noise emission (Thanedar *et al.* 2017)

Thanedar *et al.* (2017) investigated the effect of process parameter responsible for grinding burn on Barkhausen noise emission. According to them, increase in wheel speed and infeed increases the heat generation in the grinding zone leading to more Barkhausen noise emission whereas increase in work velocity reduces the time of contact between abrasive grain and workpiece resulting in lower grinding zone temperature which reduces the Barkhausen noise emission and the same is depicted in Fig.2.8.

Correa *et al.* (2016) studied the effect of annealing heat treatment and stress relieving which includes the heating of API 5L X80 steel to a temperature of 930°C for 50 minutes followed by cooling in air, water and oil. The sample were then subjected to stress relieving at a temperature of 580℃ for 2 hours and then cooling in furnace. It was noticed that sample cooled in water and not stress relieved shows lower value of Barkhausen emission due to larger dislocation density owing to presence of martensite and bainite phase. The sample under stress relief condition shows larger value of BN emission as compared to non- stress relief condition. Further, the presence of tensile residual stress modify the domain structure in such a way that it increases the movement of 180^{o} domain wall and hence increases the BN emission whereas induction of compressive residual stress restrict the motion of 180^{o} domain wall hence reduces the BN emission as can be seen from Fig.2.9.

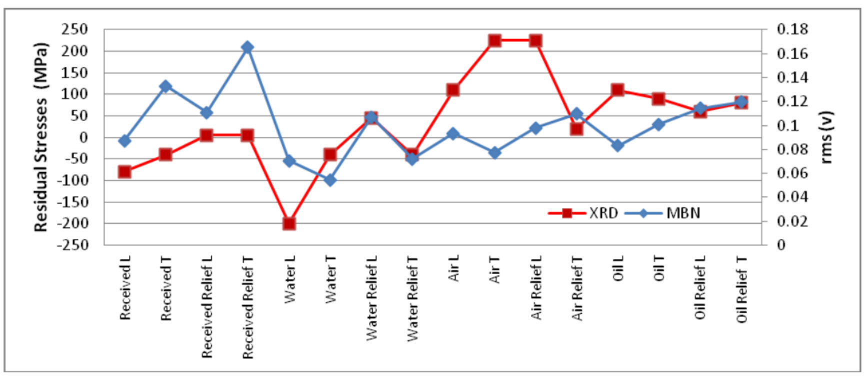

Fig.2.9 The relation between residual stress and Barkhausen emission under different condition of heat treatment (Correa *et al.*, 2016)

Vourna *et al.* (2015) studied the distribution of residual stress in the welded electrical steel using X-ray diffraction and Barkhausen noise technique. The result of the XRD shows the presence of tensile residual stress in the fusion zone whereas compressive residual stress is present in the heat affected zone of the welded sample. The Barkhausen noise measurement of the welded sample depicts that induction of tensile residual stress in the fusion zone is associated with higher value of Barkhausen emission whereas in the heat affected zone smaller BN activity is observed due to the presence of compressive residual stress. The correlation between residual stress and BN emission can be seen in Fig.2.10.

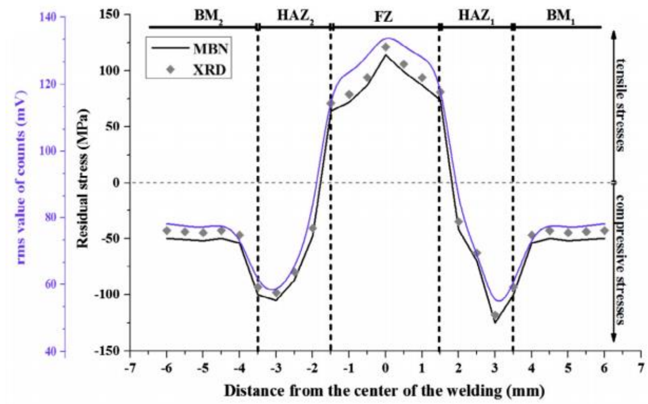

Fig.2.10 The relation between residual stress and BN emission in different zones of welded steel (Vourna *et al.*, 2015)

As discussed earlier that the presence of residual stress not only effect the Barkhausen emission rather it also have significant influence on the hysteresis loop. Piotrowski *et al.* (2017) studied the influence of plastic deformation induced residual stress on the shape of hysteresis loop. They observed that with the increase in tensile based plastic deformation, the coercivity of the sample increases whereas the steepness of the hysteresis loop decreases as can be seen from Fig.2.11 (a). However, under compression as the deformation progress, no significant changes were observed in the hysteresis loop (refer Fig.2.11 (b)).

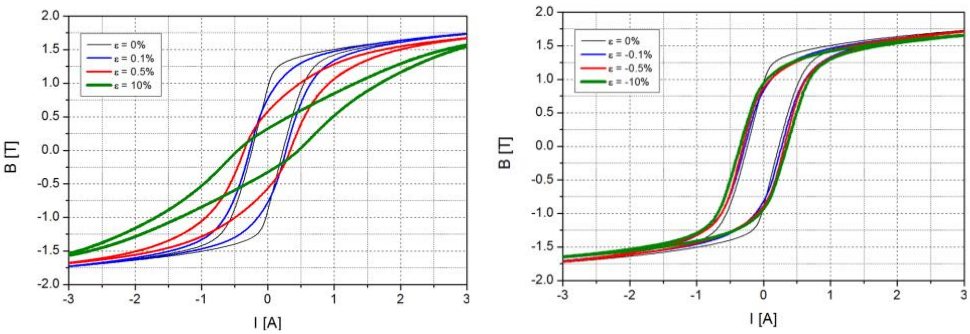

(a) (b)

Fig.2.11 Magnetic hysteresis loop for the sample subjected to (a) tensile deformation (b) compressive deformation (Piotrowski *et al.*, 2017)

Mierczak *et al.* (2011) also investigated the influence of applied stress and residual stress on the Barkhausen noise signal. But, they used reciprocal of magnetic Barkhausen noise amplitude to characterize the effect of those stresses.

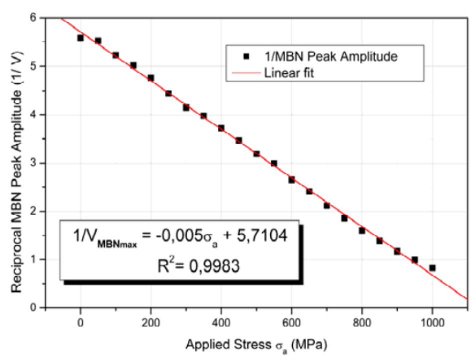

(a)

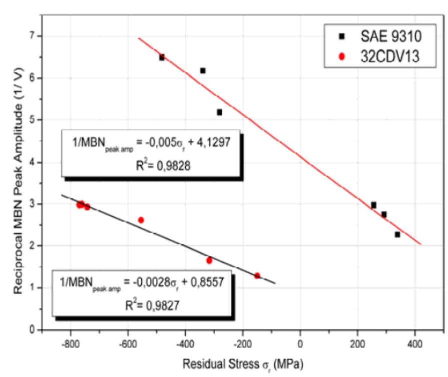

(b)

Fig.2.12 Correlation between reciprocal of MBN amplitude with (a) applied stress (b) residual stress (Mierczak *et al.* 2011)

A linear relation were observed between the reciprocal of MBN amplitude and stresses (applied and residual) as shown in Fig.2.12.

Recently, Sridharan *et al.* (2017) utilises the Barkhausen noise technique to detect distinct thermal damage occurred during grinding of bearing steel as shown in Fig.2.13. They observed a significant drop in the BN (RMS) value as the temperature exceeds 275℃ due to the occurrence of rehardening burn which tends to produce more hardness near the surface along with the presence of compressive stress due to volume expansion.

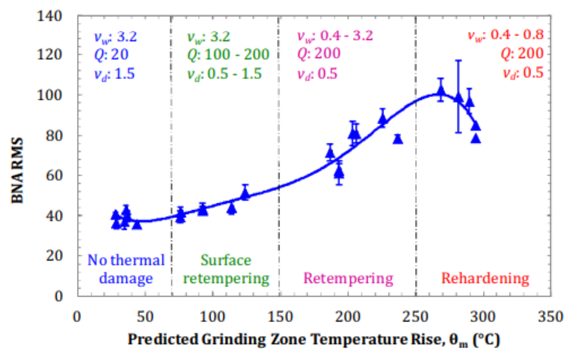

Fig.2.13 Variation in BN (RMS) with rise in grinding temperature (Sridharan *et al.*, 2017)

Vashista and Paul (2011) introduces a new parameter namely event and count of Barkhausen noise to investigate the residual stresses during grinding of hardened bearing steel. According to them previously utilised parameter like BN (RMS) is not suitable when material under investigation exhibiting poor magnetic response like hardened bearing steel. Under such condition, BN (event and count) can provide better result due to its better sensitivity towards residual stress as can be seen from Fig.2.14.

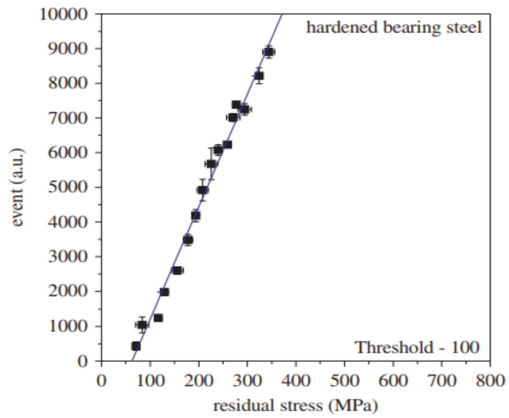

(a)

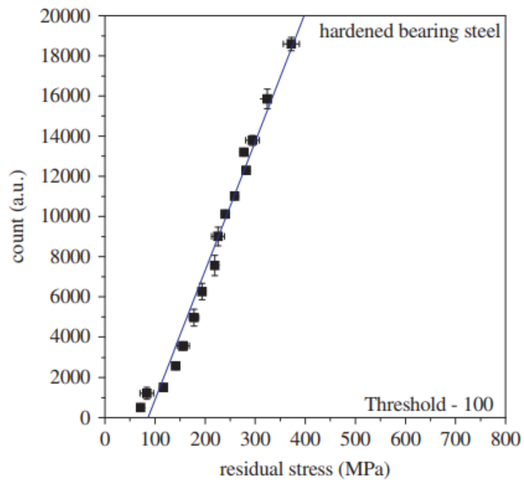

(b)

Fig.2.14 Variation in event and count with residual stress during grinding of hardened bearing steel (Vashista and Paul, 2011)

In addition to the above, a number of parameters derived from Barkhausen noise and hysteresis loop were used in the literature by various author to predict the residual stress state of the material under different manufacturing environment namely peak position and width (Blaow *et al.*, 2007), peak height (Stewart *et al.*, 2004), RMS value (Lindgren and Lepisto, 2002), MBN energy (Iordache *et al.*, 2003) and skewness (Stewart *et al.*, 2004).

2.5 Objectives

Previous work as discussed in the literature reflects the importance of surface integrity measurement and its impact on the performance of the ground product under real application. Conventional grinding technique have its own advantage and limitation over emerging high speed grinding technique but the most serious concern is the higher amount of thermal damage associated with the conventional grinding. Although a large number of technique is available to characterize such grinding damage such as metallography technique is used for white layer identification, microhardness measurement to predict hardness change on account of phase transformation, and the most important residual stresses is being evaluated using the X-ray diffraction but all these techniques are time consuming, costly and are not environmental friendly and also being laboratory based cannot be integrated in the production line to detect the damage at the rate of production.

To overcome the above issue, magnetic Barkhausen noise technique came as an alternative solution to the grinding industry which is a cost effective, less time consuming and over all can be integrated with the real manufacturing environment to detect the grinding damage at the rate of production thereby helps in lowering the production cost. But, Barkhausen noise emission is dependent on several factor including chemical composition, microstructure, hardness and residual stress state of the material and it is quite difficult to distinguish the effect of different material properties from the measured signal. Thereby, to overcome this issue the measurement devices must be calibrated with the material under investigation in order to achieve appropriate residual stress evaluation. Further, with the increase in the hardness of the material the magnetization of the material decreases which in turn reduces the sensitivity of the material properties towards Barkhausen noise emission. This imposes another level of difficulty in the characterization of material using the Barkhausen noise technique. However, extensive literature studies depicts that in spite of the above challenges the technique can be successfully utilized to assess state of stress, microstructure, plastic deformation in various metallurgical and mechanical processes. In context to grinding, the assessment of surface integrity particularly residual stress using Barkhausen noise technique is attempted by various researcher and it is important to mention here that a number of Barkhausen noise parameter (peak amplitude, RMS value, peak shift, peak position, peak width) were found to be sensitive towards residual stress. However, very few or none were studied the effect of residual stress on hysteresis loop parameter.

A thorough study of literature indicates that most of the study on Barkhausen noise is performed on material which possess good magnetization whereas few studies were undertaken on material having poor magnetization like case hardened steel. Further, the simultaneous effect of microstructure, hardness, surface roughness were not considered while evaluating the residual stress state of the material.

Hence in present study, in order to explore the application of Barkhausen noise two material one having good magnetization and other showing poor magnetization were selected. The grinding experiment were performed on both the material with variation in work velocity, downfeed, and grinding condition (dry and wet) to induce different level of surface integrity. Further, the effect of surface integrity on Barkhausen noise parameter (RMS) and also on hysteresis loop were studied in detail.

Thereby, the detailed objectives of the present investigation are as follows:

(a) to investigate the effect of various grinding parameter on different grindability indices including grinding force, temperature, specific grinding energy with particular emphasis on surface integrity (microstructure, microhardness and residual stress) while grinding low carbon steel and case hardened low carbon steel in plunge surface grinding mode.

(b) To analyze the correlation between different grindability indices and surface integrity under different grinding environment.

(c) To investigate the effect of different grinding parameter on micromagnetic response (Barkhausen noise and hysteresis loop) of the ground surface. The RMS value of the Barkhausen noise signal and average permeability derived from hysteresis loop were chosen as the micromagnetic response.

(d) To establish a possible correlation between state of residual stress of the ground surface with (RMS) value of the Barkhausen noise and newly introduced average permeability derived from hysteresis loop.